

Advances in Intelligent Systems and Computing 809

Luigi Cocchiarella *Editor*

ICGG 2018—
Proceedings of the
18th International
Conference on
Geometry and Graphics

40th Anniversary—Milan, Italy,
August 3–7, 2018



ICGG
2018



POLITECNICO
MILANO 1863

 Springer

K. Noack, D. Lordick:

Optimized Ruled Surfaces with an Application to Thin-Walled Concrete Shells.

In: L. Cocchiarella (ed): ICGG 2018 - Proceedings of the 18th International Conference on Geometry and Graphics, 40th Anniversary, Milan/Italy 2018, Springer International Publishing AG 2018, ISBN 978-3-319-95587-2, 978-3-319-95588-9 (eBook), pp. 338-349.



Optimized Ruled Surfaces with an Application to Thin-Walled Concrete Shells

Kevin Noack and Daniel Lordick^(✉)

Technische Universität Dresden, 01062 Dresden, Germany
{kevin.noack, daniel.lordick}@tu-dresden.de

Abstract. For lightweight structures in the field of architecture and civil engineering, concrete shells with negative Gaussian curvature are frequently used. One class of such surfaces are the skew ruled surfaces. To model such surfaces for the purpose of form-finding, we use the line geometry model of the Study sphere in the space of dual vectors. It allows the mapping of lines of the three-dimensional Euclidean space into points of the four-dimensional model space. The correspondence of minimal ruled surfaces, which are the helicoids, with geodesics on the dual unit sphere can be handled with the dual Rodrigues formula. This paper presents a proof of the formula and extends it to a general form, which avoids exceptions like parallel rulings. This approach also speeds up the interpolation algorithms for form-finding. The line geometry model, as implemented in Rhinoceros3D's plug-in Grasshopper, was used to design a small thin-walled footbridge of concrete in cooperation with the TU Berlin. The formwork was prepared with a hot-wire foam cutter at the TU Dresden.

Keywords: Geodesic interpolation · Dual numbers · Ruled surfaces
Rodrigues formula · Exponential mapping · Footbridge · Carbon-reinforced concrete

1 Introduction

Concrete structures typically consume lots of material and thus have a rather large carbon footprint. Therefore, building as lightweight as possible gains meaning. In this report about our ongoing research, we present a contribution to this effort. Under the premise “form follows force” the main idea is to minimize mass by using elements with a high stiffness, which results from a shape with negative Gaussian curvature. The known drawback in respect to concrete structures is the rather expensive formwork for all non-planar geometries. This drawback can be cut by a design restriction to ruled surfaces, because for this surface class, the formwork can be produced by hot-wire cutting of polystyrene foam.

In the three-dimensional Euclidean space, a ruled surface is a one-parametric smooth manifold, which can be generated by the movement of a straight line. The family of ruled surfaces can be divided in two types: the torsal ruled surfaces, which are the developable surfaces like cylinders and cones, and the skew ruled surfaces, which in general have negative Gaussian curvature, apart from single rulings, which can be

torsal. Since we want to gain high stiffness from the shapes, we concentrate on the generation of skew ruled surfaces.

Many examples for ruled surfaces can be found in architecture and civil engineering. Most prominent are the hyperbolic paraboloid, like in the work of Felix Candela, and the rotational helicoid of one sheet, like in the concrete shells of cooling towers and in the radio towers of Vladimir Shukhov. But these are only two examples out of the huge family of ruled surfaces.

For the handling of general ruled surfaces, we use a line geometry model, the dual unit sphere called the Study sphere. It is handled in the space of dual vectors with an appropriated norm. A ruled surface in the three-dimensional Euclidean space can be mapped bijectively into a curve on the Study sphere. Interestingly, a geodesic on the Study sphere corresponds to a helicoid in the Euclidean space. Since helicoids are the only non-trivial minimal ruled surfaces, geodesics are a good starting point for the design of optimized ruled surfaces.

One way to compute the geodesics is the Rodrigues formula. Its dual version leads to the method of exponential mapping which is shown in [1]. The design of minimal surfaces is explained in [2]. We show how to use the formula to validate the results of the cited papers. This includes a (short) proof that the exponential mapping can also be used in the dual vector's space.

The combination of geodesics yields only G^0 -continuous connections of surface patches. To gain smooth surfaces, an additional smoothing step is required. This can be done e.g. with an energy minimizer adjusted to dual numbers (see [3]), or with a Hermite interpolation (see [4]). Certain results of convenient interpolation algorithms shall be presented below.

The algorithms have been applied to the design of a small footbridge. It was created in cooperation with the Faculty of Civil Engineering of the TU Berlin (see [5]). The design only uses ruled surfaces. Technical basis was a combination of CAD and FEA software. The footbridge was optimized in a semi-automatic process and fabricated it with carbon-reinforced concrete. The material's thickness could be cut down to about 6 mm.

2 The Line Geometry Model: Study Sphere

This chapter presents the dual numbers and their application to line geometry. This leads to the dual unit sphere, called the Study sphere. In contrast to the Pluecker model used in [4], it generates some nice properties while acting on a sphere.

2.1 Dual Vectors

The set of real numbers \mathbb{R} is extended to the set of dual numbers

$$\mathcal{D} := \{z = a + \epsilon \cdot b \mid a, b \in \mathbb{R}, \epsilon^2 = 0\} \quad (1)$$

that form a commutative ring with the 1-element. Therefore, ϵ is the dual unit, a the primal and b the dual part. The set of dual numbers is non-ordered. This implicates an

issue in a proper definition of a minimization problem. How to treat this challenge, will be discussed later.

The (there-dimensional) dual vectors

$$l = r + \epsilon \cdot m \in \mathcal{D}^3 \tag{2}$$

are an extension of \mathcal{D} . The goal is to define a norm in the dual vector's space. Therefore, some calculation rules for the addition and multiplication of dual vectors exist:

$$l^{(1)} + l^{(2)} = \left(r^{(1)} + r^{(2)} \right) + \epsilon \cdot \left(m^{(1)} + m^{(2)} \right), \tag{3}$$

$$l^{(1)} \cdot l^{(2)} = \left(r^{(1)} \cdot r^{(2)} \right) + \epsilon \cdot \left(r^{(1)} \cdot m^{(2)} + r^{(2)} \cdot m^{(1)} \right). \tag{4}$$

The inner product is given by

$$\langle l^{(1)}, l^{(2)} \rangle = \langle r^{(1)}, r^{(2)} \rangle + \epsilon \cdot \left(\langle r^{(1)}, m^{(2)} \rangle + \langle r^{(2)}, m^{(1)} \rangle \right) \tag{5}$$

which induces the dual norm

$$\| l \|_{\mathcal{D}^3} := \| l \| = \| r \|_{\mathbb{R}^3} + \epsilon \cdot \frac{\langle r, m \rangle_{\mathbb{R}^3}}{\| r \|_{\mathbb{R}^3}}. \tag{6}$$

Dual unit vectors A line in \mathbb{R}^3 can be described by $l = p + s \cdot r$. In this model, the momentum vector $m = p \times r$, which depends on the normed direction r , replaces the local vector p . For this, the line can be represented as (l, m) in line or Pluecker coordinates. The momentum vector lies perpendicular to r , so the dual norm of a line fulfills $\| l \| = 1$. Every line corresponds to a dual unit vector. The set of all such vectors defines the dual unit sphere.

$$S_{\mathcal{D}}^2 := \{ \| l \| = 1 \mid l \in \mathcal{D}^3 \} \tag{7}$$

$S_{\mathcal{D}}^2$ is called the Study sphere. It is a submanifold of \mathcal{D}^3 . Any line in \mathbb{R}^3 can be mapped in a one-to-one correspondence to a point on $S_{\mathcal{D}}^2$. It follows that a ruled surface in \mathbb{R}^3 complies with a continuous curve on $S_{\mathcal{D}}^2$ (see Fig. 1).

For the illustration of curves lying on $S_{\mathcal{D}}^2$ in the following, there will be drawn two curves on the real unit sphere S^2 , one representing the primal and the other representing the dual part (Fig. 3).

Embedding in REAL Space Another important fact for the following algorithms is the embedding of the dual vectors into the real space $\mathcal{D}^3 \hookrightarrow \mathbb{R}^6$ defined via

$$\iota : \mathcal{D}^3 \rightarrow \mathbb{R}^6, r + \epsilon \cdot m \mapsto \begin{pmatrix} r \\ m \end{pmatrix} \tag{8}$$

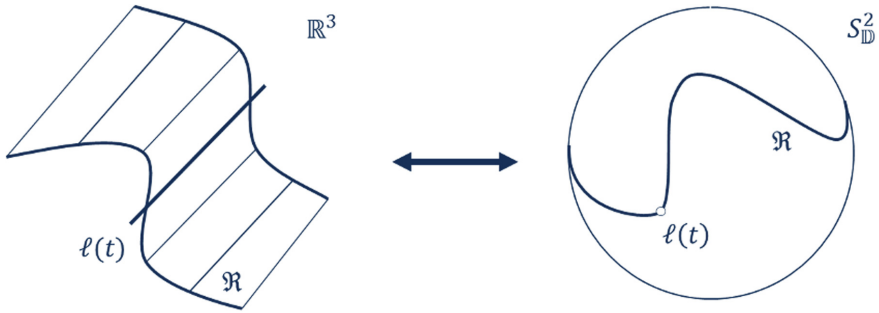


Fig. 1. Principle sketch of the two representations of a ruled surface: on the left in \mathbb{R}^3 and on the right as curve on S_D^2 (only the primal part is displayed). One ruling $l(t)$ is marked

which allows to describe the manifold of S_D^2 , denoted by $M_{S_D^2}$. Because of $m \in T_r S^2$ (tangential space), this yields $f(l) := f(\iota(l))$.

2.2 Geodesics and Minimal Ruled Surfaces

To build lightweight, a minimization problem for the desired structures has to be solved. For this purpose, we put minimal ruled surfaces already in the beginning of the algorithms. The only minimal ruled surfaces (except from the plane as the trivial case) is the helicoid. Helicoids correspond to geodesics on S_D^2 .

If a initial structure is represented by a set of rulings, those equal discrete input points on S_D^2 and can be connected by geodesics. This generates a set of helicoid patches. A critical point are the transitions between these patches. The geometrical continuity G^k for $k \in \mathbb{N}_0$ is the criteria to measure them. The kinematics in the next chapter only generates G^0 -transitions. This is very poor for technical applications (e.g. in automobile design G^3 -transitions are standard). The following interpolation algorithms are implemented to smooth the patches. A fine adjustment between the minimal surfaces and the smoothing steps brings the best results.

3 Kinematics of Rulings

Due to the lack of order in the set of dual numbers, we are not able to calculate the shortest connection between two points. So, another path is taken. Great circles can do the work on the dual unit sphere. The curve segment on a great circle between two points is a geodesic on the sphere.

In [1], the authors used the method of exponential mapping to describe the kinematics of lines. Like explained in [3], they used a one-parameter subgroup of the Lie group of dual orthogonal matrices, mapping it with the matrix exponential.

3.1 Dual Rodrigues Formula

A dual version of the Rodrigues formula generates dual geodesics on $S^2_{\mathcal{D}}$. The formula is a conclusion of Chasles' theorem, which combines a rotation with a translation to describe the kinematics of lines with a screw motion. The relation between two lines is defined by their inner product (see (5)). Another way to write it is

$$\langle l^{(1)}, l^{(2)} \rangle = \cos(\theta) - \epsilon \cdot \delta \cdot \sin(\theta) = \cos(\theta + \epsilon \cdot \delta) =: \cos(\phi) \tag{9}$$

with the real shortest distance between the lines δ and the angle between their directions θ . Together they define the dual angle ϕ (see Fig. 2). We compute θ in the known way and calculate δ with the common normal in the Hessian form.

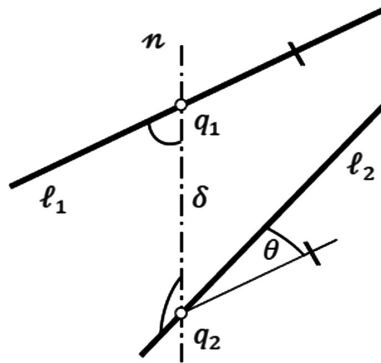


Fig. 2. Depicts two non-parallel lines. The dual angle $\phi = \theta + \epsilon \cdot \delta$ can be composed of the real-valued components: the angle between their direction θ and their distance δ . The line's cross product results in their common normal n .

The outer product brings

$$l^{(1)} \times l^{(2)} = \sin(\phi) \times n \tag{10}$$

with the common normal n between the two rulings.

The Rodrigues rotation formula describes the kinematics of lines on the Study sphere. There also exist other possibilities like dual quaternions or the Pluecker model. The research of [6] brings the dual version.

$$R(t) = I + \sin(\phi \cdot t) \cdot N + (1 - \cos(\phi \cdot t)) \cdot N^2 \tag{11}$$

With the identity matrix $I = I_3$, the dual angle ϕ , N as skew-symmetric dual matrix describing the cross product of n (representing the rotation axis), and $t \in [0, 1]$. The term $\phi \cdot t$ denotes the dual angular velocity.

Applying the rotation on the initial ruling gives the expression

$$l(t) = R(t) \cdot l^{(1)} = \sin(\phi \cdot t) \cdot (n \times l^{(1)}) + \cos(\phi \cdot t) \cdot l^{(1)} \tag{12}$$

and by using (10), we receive

$$l(t) = \frac{\sin(\phi \cdot (1 - t))}{\sin(\phi)} \cdot l^{(1)} + \frac{\sin(\phi \cdot t)}{\sin(\phi)} \cdot l^{(2)} \tag{13}$$

for the method of exponential mapping. This formula describes the motion of a line, which results in a ruled surface described by the start position $l^{(1)}$ and the end position $l^{(2)}$. If $l^{(1)}$ and $l^{(2)}$ are parallel, then $\theta = 0$ and any common normal between the rulings can be used.

With the dual Rodrigues formula, the algorithm generates geodesics on $S^2_{\mathcal{D}}$, which leads to helicoids as minimal surfaces in \mathbb{R}^3 . This method is known as the exponential mapping in the Lie group $SO(3, \mathcal{D})$ of Euclidean motions, applied for dual orthogonal matrices.

3.2 Piecewise Geodesic Interpolation

It was possible to find an extended version of Eq. (13), which allows the description of the ruling, which corresponds to the desired value of $t \in [0, 1]$. First, we have to distinguish between parallel and non-parallel rulings $l^{(1)}, l^{(2)}$. Without loss of generality, the condition $l^{(1)} \neq l^{(2)}$ holds.

Parallel control rulings For two parallel rulings $l^{(1)} = r^{(1)} + \epsilon \cdot m^{(1)}$ and $l^{(2)} = r^{(2)} + \epsilon \cdot m^{(2)}$ with $r^{(1)} = \lambda \cdot r^{(2)}$ for a $\lambda = \pm 1$, the continuous motion of $l^{(1)}$ into $l^{(2)}$ is written as

$$l(t) = \left((1 - t) \cdot r^{(1)} + t \cdot r^{(2)} \right) + \epsilon \cdot \left((1 - t) \cdot m^{(1)} + t \cdot m^{(2)} \right). \tag{14}$$

It holds $\theta = 0$ and with the dual trigonometric functions

$$\sin(\phi) = \sin(\theta) + \epsilon \cdot \delta \cdot \cos(\theta), \cos(\phi) = \cos(\theta) - \epsilon \cdot \delta \cdot \sin(\theta), \tag{15}$$

it follows $\sin(\phi \cdot t) = \epsilon \cdot \delta \cdot t$ and $\cos(\phi \cdot t) = 1$. This leads to

$$l(t) = r^{(1)} + \epsilon \cdot \left((1 - t) \cdot m^{(1)} + t \cdot m^{(2)} \right). \tag{16}$$

All rulings are parallel, so in this case the calculation creates a common plane as a (trivial) minimal surface in \mathbb{R}^3 . Nevertheless, the rulings could alternatively be connected by a helicoid.

Non-parallel control rulings The non-parallel case needs the whole set of calculation rules in the set of dual vectors. We want to extend the dual Rodrigues formula (13).

Starting again with $l^{(1)} = r^{(1)} + \epsilon \cdot m^{(1)}$ and $l^{(2)} = r^{(2)} + \epsilon \cdot m^{(2)}$ with $r^{(1)} \neq \lambda \cdot r^{(2)}$ for all $\lambda \in \mathbb{R}$, Eq. (13) is expanded to

$$l(t) = \frac{\sin((1-t)\cdot\theta) + \epsilon\cdot(1-t)\cdot\delta\cdot\cos((1-t)\cdot\theta)}{\sin(\theta) + \epsilon\cdot\delta\cdot\cos(\theta)} \cdot (r^{(1)} + \epsilon \cdot m^{(1)}) + \frac{\sin(t\cdot\theta) + \epsilon\cdot t\cdot\delta\cdot\cos(t\cdot\theta)}{\sin(\theta) + \epsilon\cdot\delta\cdot\cos(\theta)} \cdot (r^{(2)} + \epsilon \cdot m^{(2)}) \tag{17}$$

by using the relations of (15). With $\sin(\theta) \neq 0$ and the notation $A_1^{(j)} := A_1^{(j)}(t)$, especially

$$\begin{aligned} A_1^{(1)} &= \sin((1-t)\cdot\theta) \cdot \sin(\theta), \\ A_2^{(1)} &= \sin(\theta) \cdot (1-t) \cdot \delta \cdot \cos((1-t)\cdot\theta) - \sin((1-t)\cdot\theta) \cdot \delta \cdot \cos(\theta), \\ A_1^{(2)} &= \sin(t\cdot\theta) \cdot \sin(\theta), \\ A_2^{(2)} &= \sin(\theta) \cdot t \cdot \delta \cdot \cos(t\cdot\theta) - \sin(t\cdot\theta) \cdot \delta \cdot \cos(\theta), \end{aligned} \tag{18}$$

the result is

$$l(t) = \sin(\theta)^{-2} \cdot \sum_{i=1}^2 \left(A_1^{(i)} \cdot r^{(i)} + \epsilon \cdot \left(A_1^{(i)} \cdot m^{(i)} + A_2^{(i)} \cdot r^{(i)} \right) \right) \tag{19}$$

The formula (19) calculates a geodesic on S_D^2 , which corresponds to a helicoid with non-parallel rulings in \mathbb{R}^3 . The upcoming Fig. 3 illustrates that combination.

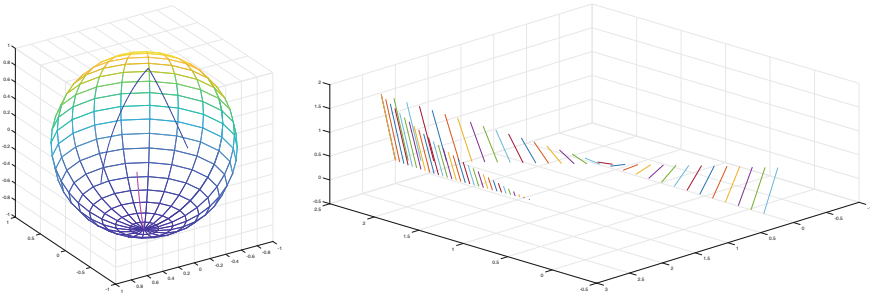


Fig. 3. Shows on the left the geodesic on S_D^2 with the primal part (pink) and the dual part (blue), computed via (19). Its representation in \mathbb{R}^3 as helicoid can be seen on the right side. Made with Matlab

The primal part of the geodesic between two parallel rulings is only a point on S_D^2 .

We want to patch geodesics in the process of piecewise geodesic interpolation for a given set of control rulings $l^{(j)}$, $j \in \mathbb{N}$. The transitions between two geodesics are G^0 -continuous. A smoothing step is needed for practical usability.

Recalculate a ruling The selection of a specific $t \in [0, 1]$ allows the identification of a corresponding point on the geodesic. In reverse we need to compute the components of the corresponding line. The unnormed direction \bar{r} (with respect to t) is given by the primal part of (19). The momentum vector $\bar{m} = \bar{p} \times \bar{r}$ can be taken from the dual part of (19). At least one component of \bar{r} does not vanish (here \bar{r}_3), so local vector's components are

$$\bar{p}_1 = -\frac{\bar{m}_2}{\bar{r}_3}, \bar{p}_2 = \frac{\bar{m}_1}{\bar{r}_3}, \bar{p}_3 = 0. \tag{20}$$

For the other two cases, we get similar results. This identification of the local vector allows a fitting illustration of the lines in \mathbb{R}^3 like in Fig. 3 (right).

4 Interpolation Algorithms

With the now validated method of exponential mapping, algorithms using minimal surfaces interpolate shells or certain geometries. The mathematical footing is set. A problem in this method lies in the transitions. They are just G^0 -continuous, which is (far) to less for technical applications. Many technical applications demand smooth transitions. Therefore, interpolation algorithms, which use smoothing splines, come to play. But by doing this, the technical-optimal solution loses the property of minimality in the sense of surface area. The smoothing algorithms in this chapter will present methods to adjust a good compromise between minimality and continuity.

Smoothing Spline via energy minimizer A first smoothing attempt would be the energy minimizer, applied to S^2_D (see [3]), to interpolate with the beneficial slightest oscillation. For a given set of strictly monotonically increasing timestamps $t_i \in [0, 1]$ and points $q_i \in M_{S^2_D}$, a smoothing spline γ_s solves the curve-fitting problem.

$$S(\gamma) := \sum_{i=1}^m \|\gamma(t_i) - q_i\|^2 + \frac{\lambda_1}{2} \cdot \int_0^1 \|\dot{\gamma}(t)\|^2 dt + \frac{\lambda_2}{2} \cdot \int_0^1 \|\ddot{\gamma}(t)\|^2 dt. \tag{21}$$

It should be minimized for fixed non-negative λ_1, λ_2 as boundary value problem. The result of the smoothed geometry in comparison to helicoid patches, computed via exponential mapping, can be seen in Fig. 4 in \mathbb{R}^3 .

Global geodesic interpolation A global smoothing step over all control rulings would lead to a helicoid that is minimal but, in general, only touches the first and last control ruling. This is a good way if the control rulings are close together, so that the designed shape of ruled surfaces has a small oscillation. Otherwise, some problems can occur. If we take for example three orthogonal control lines, then the global geodesic will have a pretty different behavior than the two local geodesics (see Fig. 5). We get rid of the transitions but lose some properties of the originally form.

The use of Bézier splines is not recommended. They oscillate too much to fulfill sufficiently the claim of minimality. Another option would be a dynamic relaxation of

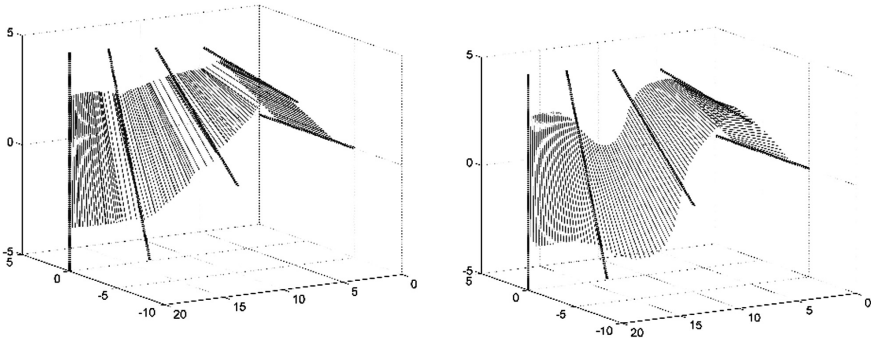


Fig. 4. Helicoids, designed with the method of exponential mapping on the left and the smoothing spline on the right side. Cited from [3]

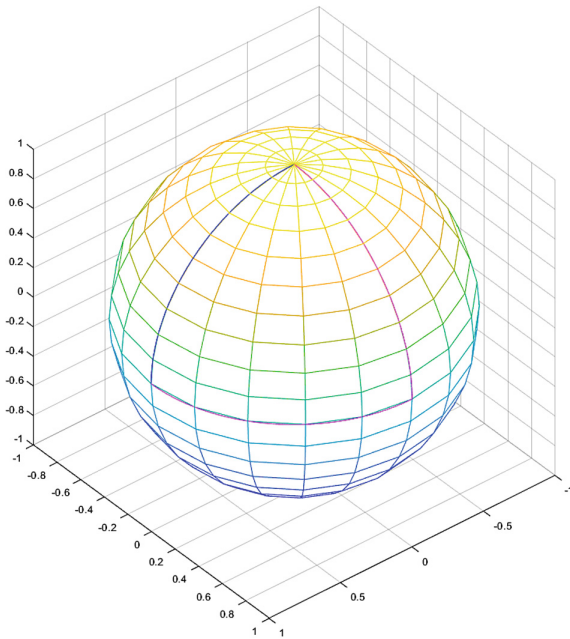


Fig. 5. The image contains a simple problematic example of global geodesic interpolation between the first and last control ruling on S^2_D : the lose some main properties of the ruled surfaces. Here, only the primal part of three orthogonal rulings are displayed

the helicoid patches. More information about this can be found in [7]. We implemented the common algorithms and could speed them up by using the Eqs. (16) and (19) instead of working with the matrix exponential of [1].

5 Building the Footbridge

In cooperation with the group of Prof. Mike Schlaich at the Faculty of Civil Engineering of the TU Berlin a small footbridge became the testing field for the mentioned algorithms (Fig. 6). Starting from an idea of Mike Schlaich, the bridge was created as a shell-like structure from carbon reinforced concrete, composed of patches of skew ruled surfaces.

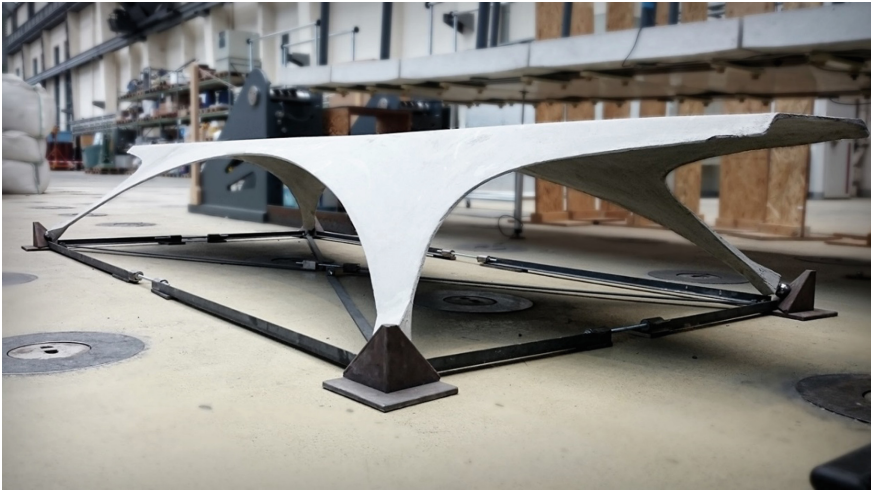


Fig. 6. The prototype of a footbridge made of carbon-reinforced concrete. It was designed with line geometry tools developed for the Rhinoceros3D plug-in Grasshopper and with the FEA software SOFiSTiK

Design model For the design of the footbridge the tools built upon the line geometry model have been used. In conjunction with the FEA software SOFiSTiK, an optimization with respect to the load and stress distribution on the bridge was done properly. As a result of it, the bridge was fabricated out of concrete with a thickness down to about 6 mm. The whole process was iterative and semi-automatic.

Fabrication of the prototype The production process was split in different stages at different locations. After the CAD and FEA design, for each element of the bridge (see Fig. 7) the CAD data was converted into G-Code. Then the formwork from polystyrene foam was made in Dresden by means of a hot-wire cutter. Unfortunately, the work with the cutter was rather slow and less accurate than expected. The initial goal was to realize a shell thickness of 5 mm. But we had to fight with tolerances of about 3 mm. The formwork elements have then been transported to Berlin. There, in preparation of the molding, a substructure was erected for the polystyrene foam segments. Finally the concrete, reinforced with carbon, was poured and filled.

The footbridge prototype was presented at the Footbridge Conference 2017 in Berlin and tested for a load of 300 kg without failure.

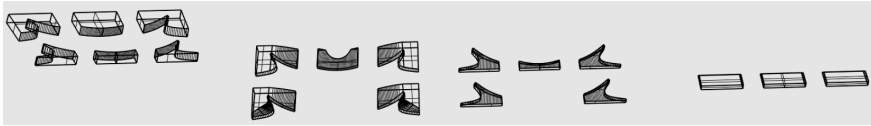


Fig. 7. The composition of 19 parts leads to the footbridge, each one consisting of ruled surfaces. They have to be cut separately with the hot-wire cutter and patched together for the concreting

6 Conclusions

For the form-finding of ruled surfaces a line geometry model in the space of dual vectors, the Study sphere, was used. In this context the one-to-one correspondence between ruled surfaces in \mathbb{R}^3 and continuous curves on the Study sphere S_D^2 proved to be a helpful tool.

The core of the used algorithms is the computation of geodesics on the Study sphere, which correspond to the only minimal ruled surfaces, the helicoids. The underlying Rodrigues formula was extended to validate the procedure of the exponential mapping.

If a set of rulings is used as an input, this triggers a piecewise geodesic interpolation on the Study sphere. The result of this starting algorithm is a set of helicoids with C^0 -continuity.

There are several approaches to smooth the piecewise geodesic interpolation. One option is to use an energy minimizer on the Study sphere. We were able to speed up existing intersection and relaxation algorithms with the extension of the dual Rodrigues formula.

In cooperation with the Faculty of Civil Engineering of the TU Berlin a footbridge was designed, consisting completely of ruled surface patches. A process combining CAD and FEA software led to an optimized form. This was done with respect to minimal material consumption and an efficient stress and load distribution. It was possible to bring the concrete's thickness down to 6 mm.

Further research could include other spline techniques like Hermite interpolation (see [4]) or centered thin plate splines in Riemannian manifolds (see [8]) to get smooth transition between the patches with less effort. Another open topic is the identification of specific points on a line in combination with the Study sphere model. This is a requirement to implement finite elements methods directly into the line geometry model.

It is planned to publish the interpolation methods as an add-on to the Grasshopper plug-in in the CAD software Rhinoceros3D. A presentation and exploration of the methods within a design summer school 2018 in Dresden is in preparation.

Acknowledgements. This work is part of the research project “Thin-walled Concrete Structures with Line Geometry” funded by the German Research Foundation (DFG) as part of the SPP 1542. Two theses at the TU Berlin by Jakob Grave (master thesis) and Jonas Klages (bachelor thesis) contributed to the realization of the footbridge prototype. The formwork was prepared at the Makerspace of the Saxon State and University Library in Dresden (SLUB).

References

1. Sprott, K., Ravani, B.: Kinematic generation of ruled surfaces. *Adv. Comput. Math.* **17**(1–2), 115–133 (2002)
2. Hagemann, M., Klawitter, D., Lordick, D.: Force driven ruled surfaces. *J. Geom. Graph.* **17**(2), 193–204 (2013)
3. Pott, M., Lordick, D.: Dual spherical energy minimizer with applications to smoothing splines. In: 17th International Conference on Geometry and Graphics, Beijing (2016)
4. Odehnal, B.: Hermite interpolation of ruled surfaces and channel surfaces (2017)
5. Osman Letelier, J.P., Goldack, A., Schlaich, M., Lordick, D., Grave, J.: Shape optimization of concrete shells with ruled surface geometry using line geometry. In: International Association for Shells and Spatial Structures: IASS Annual Symposium, Hamburg (2017)
6. Hagemann, M., Klawitter, D.: Discretisation of light-weight concrete elements using a line-geometric model. In: Proceedings of the 9th fib International PhD Symposium in Civil Engineering, pp. 269–274. KIT Scientific Publishing, Karlsruhe (2012)
7. Klawitter, D., Hagemann, M., Odehnal, D.: Curve flows on ruled surfaces. *J. Geom. Graph.* **17**(2), 129–140 (2013)
8. Varano, V., Gabriele, S., Teresi, L., Dryden, I.L., Puddu, P.E., Torromeo, C., Piras, P.: The TPS direct transport: a new method for transporting deformations in the size-and-shape space. *Int. J. Comput. Vis.* **124**(3), 384–408 (2017)
9. Pottmann, H., Wallner, J.: *Computational Line Geometry*. Springer, Heidelberg (2001)
10. Lordick, D.: Intuitive design and meshing of non-developable ruled surfaces. In: Proceedings of the Design Modelling Symposium Berlin, pp. 248–261, University of the Arts Berlin (2009). URL <http://lordick.dgfgg.de/docs/DMSB2009-Lordick-150.pdf>
11. Lordick, D., Klawitter, D., Hagemann, M.: Liniengeometrie für den Leichtbau. In: Scheerer, S., Curbach, M. (Hrsg.): *Leicht Bauen mit Beton—Forschung im Schwerpunktprogramm 1542 Förderphase I*, pp. 224–235. TU Dresden, Dresden (2014)
12. Schlaich, J.: Conceptual design of light structures. *J. Int. Assoc. Shells Spat. Struct.: IASS* **45**, 157–168 (2004)
13. Odehnal, B.: Subdivision algorithms for ruled surfaces. *J. Geom. Graph.* **12**(1), 1–18 (2008)
14. Firl, M.: Optimal shape design of shell structures. Dissertation, München (2010). URL <http://mediatum.ub.tum.de/doc/981720/512948.pdf>
15. Bletzinger, K.-U., Wüchner, R., Daoud, F., Camprubí, N.: Computational methods for form finding and optimization of shells and membranes. *Comput. Methods Appl. Mech. Eng.* **194**(30), 3438–3452 (2005)
16. Ramm, E., Bletzinger, K.-U.: Computational form finding and optimization. In: Adrienssens, S., Block, P., Veenendaal, D., Williams, C. (Hrsg.): *Shell Structures for Architecture. Form Finding and Optimization*, pp. 45–55. Taylor, Hoboken (2014)
17. Pottmann, H., Peternell, M., Ravani, B.: Introduction to line geometry with applications. *CAD Comput. Aided Des.* **31**, 3–16 (1999)
18. Kemmler, R.: Große Verschiebungen und Stabilität in der Topologie- und Formoptimierung. Dissertation, Stuttgart (2004). URL https://www.ibb.uni-stuttgart.de/publikationen/fulltext_new/2004/kemmler-2004.pdf
19. Hofer, M., Pottmann, H.: Energy-minimizing splines in manifolds. *ACM Trans. Graph.* **23**(3), 284 (2004)
20. Absil, P.-A., Mahony, R., Sepulchre, R.: *Optimization algorithms on matrix manifolds*. Princeton University Press, Princeton, NJ (2008)